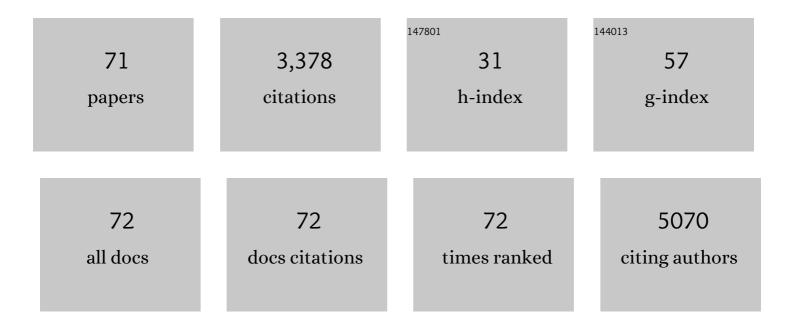
Lidong Sun

List of Publications by Year in descending order

Source: https://exaly.com/author-pdf/8257129/publications.pdf Version: 2024-02-01



#	Article	IF	CITATIONS
1	Efficient demulsification of ultralow-concentration crude oil-in-water emulsion by three-dimensional superhydrophilic channels. Science China Materials, 2022, 65, 213-219.	6.3	10
2	Alteration of freezing paradigms of an impact water droplet on different cold surfaces. International Journal of Heat and Mass Transfer, 2022, 183, 122177.	4.8	7
3	Conformally anodizing hierarchical structure in a deformed tube towards energy-saving liquid transportation. Chemical Engineering Journal, 2022, 431, 133746.	12.7	1
4	Dissecting the Chain Length Effect on Separation of Alkane-in-Water Emulsions with Superwetting Microchannels. ACS Applied Materials & Interfaces, 2022, 14, 6157-6166.	8.0	6
5	Recent advances in high-performance membranes for vanadium redox flow battery. , 2022, , 131-154.		0
6	Polytetrafluoroethylene Modified Nafion Membranes by Magnetron Sputtering for Vanadium Redox Flow Batteries. Coatings, 2022, 12, 378.	2.6	2
7	Percolative Anodization: Tailoring TiO ₂ Nanotube Arrays Inside Ultrafine Ti Microchannels. Journal of the Electrochemical Society, 2022, 169, 046517.	2.9	1
8	Recent developments in slippery liquid-infused porous surface. Progress in Organic Coatings, 2022, 166, 106806.	3.9	21
9	A cost-effective nafion/lignin composite membrane with low vanadium ion permeation for high performance vanadium redox flow battery. Journal of Power Sources, 2021, 482, 229023.	7.8	113
10	Unique dynamics of water-ethanol binary droplets impacting onto a superheated surface with nanotubes. International Journal of Heat and Mass Transfer, 2021, 164, 120571.	4.8	13
11	Fluorinated graphene nanoribbons from unzipped single-walled carbon nanotubes for ultrahigh energy density lithium-fluorinated carbon batteries. Science China Materials, 2021, 64, 1367-1377.	6.3	38
12	Recent advances in photocatalytic decomposition of water and pollutants for sustainable application. Chemosphere, 2021, 276, 130201.	8.2	32
13	The effects of TiO2 nanotubes on the biocompatibility of 3D printed Cu-bearing TC4 alloy. Materials and Design, 2021, 207, 109831.	7.0	17
14	TiO2/CuS core-shell nanorod arrays with aging-induced photoelectric conversion enhancement effect. Electrochemistry Communications, 2020, 111, 106648.	4.7	10
15	Film levitation and central jet of droplet impact on nanotube surface at superheated conditions. Physical Review E, 2020, 102, 043108.	2.1	10
16	Highly Stable Vanadium Redoxâ€Flow Battery Assisted by Redoxâ€Mediated Catalysis. Small, 2020, 16, e2003321.	10.0	65
17	Hybrid Membranes Dispersed with Superhydrophilic TiO ₂ Nanotubes Toward Ultra‣table and Highâ€Performance Vanadium Redox Flow Batteries. Advanced Energy Materials, 2020, 10, 1904041.	19.5	115
18	Conformal Filling of TiO 2 Nanotubes with Dense M x S y Films for 3D Heterojunctions: The Anion Effect. ChemElectroChem, 2019, 6, 1177-1182.	3.4	10

LIDONG SUN

#	Article	IF	CITATIONS
19	The pivotal effects of oxygen vacancy on Bi2MoO6: Promoted visible light photocatalytic activity and reaction mechanism. Chinese Journal of Catalysis, 2019, 40, 647-655.	14.0	86
20	Reversibly tuning the surface state of Ag via the assistance of photocatalysis in Ag/BiOCl. Nanotechnology, 2019, 30, 305601.	2.6	16
21	A Bi/BiOI/(BiO)2CO3 heterostructure for enhanced photocatalytic NO removal under visible light. Chinese Journal of Catalysis, 2019, 40, 362-370.	14.0	63
22	Biotemplate derived three dimensional nitrogen doped graphene@MnO2 as bifunctional material for supercapacitor and oxygen reduction reaction catalyst. Journal of Colloid and Interface Science, 2019, 544, 155-163.	9.4	63
23	A nanopump for low-temperature and efficient solar water evaporation. Journal of Materials Chemistry A, 2019, 7, 24311-24319.	10.3	34
24	A green SPEEK/lignin composite membrane with high ion selectivity for vanadium redox flow battery. Journal of Membrane Science, 2019, 572, 110-118.	8.2	153
25	A solar tube: Efficiently converting sunlight into electricity and heat. Nano Energy, 2019, 55, 269-276.	16.0	50
26	Room-temperature up-conversion random lasing from CsPbBr ₃ quantum dots with TiO ₂ nanotubes. Optics Letters, 2019, 44, 4706.	3.3	14
27	Effect of Electrolyte Pretreatment on the Formation of TiO ₂ Nanotubes: An Ignored yet Nonâ€negligible Factor. ChemElectroChem, 2018, 5, 1006-1012.	3.4	17
28	Enhanced photocatalytic activity induced by sp3 to sp2 transition of carbon dopants in BiOCl crystals. Applied Catalysis B: Environmental, 2018, 221, 467-472.	20.2	58
29	General Way To Compute the Intrinsic Contact Angle at Tubes. Journal of Physical Chemistry C, 2018, 122, 29210-29219.	3.1	21
30	Ion Selectivity and Stability Enhancement of SPEEK/Lignin Membrane for Vanadium Redox Flow Battery: The Degree of Sulfonation Effect. Frontiers in Chemistry, 2018, 6, 549.	3.6	21
31	Nanostructured Three-Dimensional Percolative Channels for Separation of Oil-in-Water Emulsions. IScience, 2018, 6, 289-298.	4.1	44
32	Electric-field control of magnetism in a few-layered van der Waals ferromagnetic semiconductor. Nature Nanotechnology, 2018, 13, 554-559.	31.5	466
33	Performance improvement of perovskite solar cells through enhanced hole extraction: The role of iodide concentration gradient. Solar Energy Materials and Solar Cells, 2018, 185, 117-123.	6.2	176
34	SPEEK Membrane of Ultrahigh Stability Enhanced by Functionalized Carbon Nanotubes for Vanadium Redox Flow Battery. Frontiers in Chemistry, 2018, 6, 286.	3.6	49
35	Surface Reorganization Leads to Enhanced Photocatalytic Activity in Defective BiOCl. Chemistry of Materials, 2018, 30, 5128-5136.	6.7	55
36	Evolution of Oxyhalide Crystals under Electron Beam Irradiation: An in Situ Method To Understand the Origin of Structural Instability. Inorganic Chemistry, 2018, 57, 8988-8993.	4.0	15

LIDONG SUN

#	Article	IF	CITATIONS
37	Towards high efficiency thin film solar cells. Progress in Materials Science, 2017, 87, 246-291.	32.8	85
38	Conductivity Enhancement of PEDOT:PSS via Addition of Chloroplatinic Acid and Its Mechanism. Advanced Electronic Materials, 2017, 3, 1700047.	5.1	126
39	Coaxial anodic oxidation under dynamic electrolyte conditions for inner surface patterning of high-aspect-ratio and slim Ti tubes. Corrosion Science, 2017, 124, 193-197.	6.6	22
40	Large-Scale, Uniform, and Superhydrophobic Titania Nanotubes at the Inner Surface of 1000 mm Long Titanium Tubes. Journal of Physical Chemistry C, 2017, 121, 15448-15455.	3.1	43
41	Robust Cesium Lead Halide Perovskite Microcubes for Frequency Upconversion Lasing. Advanced Optical Materials, 2017, 5, 1700419.	7.3	64
42	Unique lift-off of droplet impact on high temperature nanotube surfaces. Applied Physics Letters, 2017, 111, .	3.3	26
43	Growth of NiMn LDH nanosheet arrays on KCu ₇ S ₄ microwires for hybrid supercapacitors with enhanced electrochemical performance. Journal of Materials Chemistry A, 2017, 5, 20579-20587.	10.3	116
44	Inverted Planar Perovskite Solar Cells with a High Fill Factor and Negligible Hysteresis by the Dual Effect of NaCl-Doped PEDOT:PSS. ACS Applied Materials & Interfaces, 2017, 9, 43902-43909.	8.0	149
45	Towards high-performance transistors and photodetectors with monolayer graphene through modified transfer and lithography process. Materials Express, 2017, 7, 230-236.	0.5	2
46	Interdigitated CuS/TiO2 Nanotube Bulk Heterojunctions Achieved via Ion Exchange. Electrochimica Acta, 2016, 199, 180-186.	5.2	17
47	Employing ZnS as a capping material for PbS quantum dots and bulk heterojunction solar cells. Science China Materials, 2016, 59, 817-824.	6.3	14
48	Size-dependent crystalline fluctuation and growth mechanism of bismuth nanoparticles under electron beam irradiation. Nanoscale, 2016, 8, 12282-12288.	5.6	19
49	Nanocomposites of AgInZnS and graphene nanosheets as efficient photocatalysts for hydrogen evolution. Nanoscale, 2015, 7, 18498-18503.	5.6	23
50	Cuprous sulfide counter electrodes prepared by ion exchange for high-efficiency quantum dot-sensitized solar cells. Journal of Materials Chemistry A, 2014, 2, 2807.	10.3	63
51	Anodic Titania Nanotubes Grown on Titanium Tubular Electrodes. Langmuir, 2014, 30, 2835-2841.	3.5	35
52	Ultralong, Small-Diameter TiO ₂ Nanotubes Achieved by an Optimized Two-Step Anodization for Efficient Dye-Sensitized Solar Cells. ACS Applied Materials & Interfaces, 2014, 6, 1361-1365.	8.0	37
53	PbS Quantum Dots Capped with Amorphous ZnS for Bulk Heterojunction Solar Cells: The Solvent Effect. ACS Applied Materials & Interfaces, 2014, 6, 14239-14246.	8.0	26
54	Conformal Growth of Anodic Nanotubes for Dye-Sensitized Solar Cells: Part II. Nonplanar Electrode. Journal of Nanoscience and Nanotechnology, 2014, 14, 2050-2064.	0.9	12

LIDONG SUN

#	Article	IF	CITATIONS
55	PbS Quantum Dots Embedded in a ZnS Dielectric Matrix for Bulk Heterojunction Solar Cell Applications. Advanced Materials, 2013, 25, 4598-4604.	21.0	50
56	A composite electrode of TiO2 nanotubes and nanoparticles synthesised by hydrothermal treatment for use in dye-sensitized solar cells. RSC Advances, 2013, 3, 11001.	3.6	11
57	On seeding of the second layer in growth of double-layered TiO2 nanotube arrays. Electrochimica Acta, 2013, 107, 200-208.	5.2	17
58	Fabrication of TiO ₂ /CuSCN Bulk Heterojunctions by Profile-Controlled Electrodeposition. Journal of the Electrochemical Society, 2012, 159, D323-D327.	2.9	25
59	Conformal Growth of Anodic Nanotubes for Dye-Sensitized Solar Cells: Part I. Planar Electrode. Nanoscience and Nanotechnology Letters, 2012, 4, 471-482.	0.4	16
60	A novel parallel configuration of dye-sensitized solar cells with double-sided anodic nanotube arrays. Energy and Environmental Science, 2011, 4, 2240.	30.8	42
61	Transition from Anodic Titania Nanotubes to Nanowires: Arising from Nanotube Growth to Application in Dyeâ€Sensitized Solar Cells. ChemPhysChem, 2011, 12, 3634-3641.	2.1	21
62	A Two-step anodization to grow high-aspect-ratio TiO2 nanotubes. Thin Solid Films, 2011, 519, 4694-4698.	1.8	39
63	Effect of the Geometry of the Anodized Titania Nanotube Array on the Performance of Dye-Sensitized Solar Cells. Journal of Nanoscience and Nanotechnology, 2010, 10, 4551-4561.	0.9	77
64	Double-Sided Anodic Titania Nanotube Arrays: A Lopsided Growth Process. Langmuir, 2010, 26, 18424-18429.	3.5	30
65	Anodized Titania Nanotube Array and its Application in Dye-Sensitized Solar Cells. , 2010, , 57-108.		0
66	Effect of electric field strength on the length of anodized titania nanotube arrays. Journal of Electroanalytical Chemistry, 2009, 637, 6-12.	3.8	79
67	High temperature oxidation behavior of hafnium modified NiAl bond coat in EB-PVD thermal barrier coating system. Thin Solid Films, 2008, 516, 5732-5735.	1.8	118
68	Three surface modification methods and their effects on the isothermal oxidation behavior of the EB-PVD NiAl coating. Surface and Coatings Technology, 2007, 201, 5161-5164.	4.8	8
69	Element diffusion during fabrication of EB-PVD NiAl coating and its 1100°C isothermal oxidation behavior (II). Surface and Coatings Technology, 2007, 201, 6589-6592.	4.8	20
70	Phosphatidylinositol 3-kinase/protein kinase B pathway stabilizes DNA methyltransferase I protein and maintains DNA methylation. Cellular Signalling, 2007, 19, 2255-2263.	3.6	73
71	How to Compute the Contact Angle inside an Opaque Capillary Tube: A Universal Equation. Advanced Theory and Simulations, 0, , 2100474.	2.8	0